



# Path Scheduling and Target Trajectory Optimization in UAVs based on Dragonfly and Firefly Algorithm

Methaq Hadi Lafta<sup>1,\*</sup>

<sup>1</sup> Iraqi Ministry of Education

## Highlights

- Dragonfly/Firefly algorithm applies, owing to no real-time tracing and path scheduling
- LQG controller and 3D Kalman filter are part of the UAV tracking route
- The simulation indicates that the UAV's power consumption is equivalent to 56.2045 MW
- This study will use MSE, PSNR, SNR, and Accuracy Criteria as evaluation criteria.

## Article Info

Received: 15 August 2022  
 Received in revised: 03 October 2022  
 Accepted: 03 October 2022  
 Available online: 04 October 2022

## Keywords

UAVs,  
 Path Scheduling,  
 Target Trajectory,  
 LQG Controller,  
 Dragonfly Algorithm,  
 Firefly Algorithm

## Abstract

It is hoped that there will never be a war in the world, but one of the defensive requirements of any country during the war is the using Unmanned Aerial Vehicle used for destruction and defense. Today, UAVs movement from origin to destination is an important problem due to the abundant application of UAVs in wars and experimental research. This is important because the range of some UAVs in fly time is low, and others are very high due to their fuel. Parametric indeterminacy is several factors in UAVs movement prediction and trajectory, such as speed, movement angle, accuracy, movement time, and situation and direct control. So, this research is trying to provide a method based on LQG controller with and then set motion and specify path scheduling without deviations based on swarm intelligence algorithms in combinational mode: Dragonfly-Firefly algorithm. The simulation results showed that the UAV power consumption is comparable to 56.2045 MW, which signifies a prosperous pass. Mean Square Error, Peak Signal to Noise Ratio, Signal-to-Noise Ratio, and Accuracy Criteria will all be used in this study. Based on the results of the evaluation criteria, it is feasible to ensure that the recommended technique will be used for UAV route scheduling and target trajectory optimization when the project is finished.

## Nomenclature

ACO	Ant Colony Optimizer	PKF	Particle Kalman Filter
CKF	Cubature Kalman Filters	PSO	Particle Swarm Optimization
DEA	Differential Evolution Algorithm	PSNR	Peak Signal to Noise Ratio
3DKF	3D Kalman Filter	PPF	Prescribed Performance Function
EKF	Extended Kalman Filter	RISE	Robust Integral of the Signum of the Error
GA	Genetic Algorithm	SNR	Signal-to-Noise Ratio
HAS	Harmony Search Algorithm	SMO	Sequential Minimum Optimization
LKF	Linear Kalman Filter	UAV	Unmanned Aerial Vehicle
LSTM	Long Short-Term Memory	UKF	Unscented Kalman Filter

\* Corresponding Author: Methaq Hadi Lafta  
 Email: [Mithaqiraqi@gmail.com](mailto:Mithaqiraqi@gmail.com)

## 1. Introduction

Mobile Robots such as UAVs scheduling is an efficient method for preventing probabilistic errors for collision. In recent years, routing and path scheduling algorithms have been used in various applications. Based on different search techniques, such as decisive and random search, path scheduling algorithms are divided into two categories. Decisive search methods include dynamic programming, such as Astar (A\*) method, but evolutionary algorithms are used in random search methods, such as Genetic and PSO algorithms [1]. The optimal route collects information directly by a connected line using greedy and evolutionary algorithms in a set of path stations in 3d space. So, the initial path of these algorithms produces a broken line. However, UAVs cannot accurately determine a schedule with a broken line because of the limitation of dynamic performance and UAVs kinematic features. The main purpose of path scheduling is tracking to produce a distinct path in which the radius of curvature is greater than the minimum radius of rotation at any point, and the path should identify the continuity of the curve [1].

In general, tracking the UAVs involve identifying targets from launch to target time. Meanwhile, the identification of movement parameters such as speed, angle of movement, accuracy, time of movement, positioning, and localization of the head and the bottom of the UAVs as direct movement is important, which is the main challenge of this research for target trajectory. Hence, a large study area for military and aeronautical applications is being made for UAVs tracking and other moving objects. Typically, the dimensions first obtained to track the objectives of moving UAVs by a sensor in the polar coordinates of the UAVs are reported, then modeled by Cartesian coordinates. For this job, Kalman filters are appropriate. The Kalman filter is a filter that can detect noise as a variable, estimate errors and possible errors, and also estimate unknown variables that tend to be accurate. To do this, there are several Kalman filter models, including LKF, EKF, WSKF, PKF, 3d KF, UKF, and CKF.

In tracking the path, assuming that the UAVs parameters change and this change is done linearly, Kalman filter equations that can be overcome this issue. Because the simulation world (the continuous world) is different from the real world (the discrete world), the same parameters should be used to implement the proposed method that tracks the UAVs until it encounters the target and between track-to-target tracking it will be done. Hence, the Kalman filter which has more similarities to the discrete world is a three-dimensional Kalman filter that is

considered in this study. Because the environment in which the UAVs move is 3D and the Kalman filter, which can track target operations by specifying parameters such as speed, angle of movement, precision, movement time, position is three-dimensional Kalman filter which has higher capacities than other Kalman filters, including the Extended Kalman filter and the Without Sequencing Kalman filter.

It should be noted at the outset that the parameters of the UAVs, including its position, speed, and initial motion angle are set manually and for which purpose it is determined and these parameters change until reaching that goal. Output noise data is the sensor which sends the information to the controller. In fact, there is also a controller in the UAVs that can be controlled by any model. The purpose of this study is to use the LQG controller.

One of the reasons for using the 3D Kalman filter is as follows: tracking the path, assuming that the parameters of the UAVs are changed and this change is done linearly, so that Kalman filters can be used to overcome these problems. The three-dimensional Kalman filter parameters to reach the target in this research include a number of important items which include the position of the UAVs, the UAVs velocity at run-time, the time-per-second, and time-varying velocity update at different time intervals along the movement, UAVs control to track the target, and prevent collisions with other objects (barrier detection). These parameters cannot be fully and correctly optimized with Kalman filters. Now why are we considering space as NP-Hard, because to this day the correct and accurate approach has not been scientifically presented in the articles, and therefore the use of evolutionary algorithms and swarm intelligence can be optimized for this space.

The method of path scheduling and target trajectory to reach the intended purpose of this research is to use random search methods. Since the Genetic algorithm has high convergence and speed, another same family algorithms that are swarm intelligence, have a higher rate of improvement than evolutionary algorithms. Hence, the use of a Dragonfly-Firefly Algorithm as combination mode will be used to optimize the 3D Kalman filter. The Dragonfly-Firefly Algorithm is very effective in conditions with a very large search space compared to conditions with small search space and is very effective in optimizing it due to its non-singular characteristics. The two most important factors in this algorithm include the attractiveness and intensity of light. Methods for reaching the target state estimation to describe the dynamic state of the UAVs to reach the target will be considered including equivalent

noise, detection and input along with switching. Considering the time, speed, movement and changing model are vital that according to the definitions given by Kalman filters and its Three-Dimensional type by optimizing it in a large space with the Dragonfly-Firefly Algorithm and these challenges are fixed.

In the following, in addition to considering the method outlined in [1], it is necessary to consider some other similar methods that will be considered as base articles. In [2], the selection of the self-adaptive parameter is used with a prediction approach using a Hidden Markov Model<sup>2</sup> algorithm for a moving object. Also, in [3], dynamical analysis and path tracking are used by calculating the torque method optimally for a moving robot. In [4], the Kalman filter has been developed to detect rockets that consider parameters such as position and velocity to reach the target as critical research parameters that have been performed well. The rest of this paper organized as follows. In part two, an overview of UAVs controller in path scheduling and target trajectory surveyed. Based on some issues in recent and previous models and methods, part three describe and formulate a new method for UAVs controller in path scheduling and target trajectory. After that in part four, a simulation done in MATLAB environment by analyzing outputs. At the end, part six, reviewed this article by conclusion.

## 2. Literature Review

Numerous scholars have looked at the issue of autonomous target tracking from various angles as a result of the expanding use of space science and communications. Based on the target energy emitted, the radar tracking system typically determines the missile's direction towards the target. In the face of deceptive fighter behavior that affects the creation of navigation commands, these systems are frequently forced to diagnose a legitimate target. In general, there are three types of routing in missiles: flat routing, hierarchical routing, and routing of a place that depends on a network. A routing strategy based on network structure is employed in this study.

For each missile to forecast its trajectory, a controller is required. Controlling a system requires gathering, analyzing, and sending the proper commands to the functional components that power the system. A missile's controller is comparative, and there are typically three different forms of comparative controllers: benefit tabulation, comparative control of the reference model, and self-regulating regulators. In this study, self-regulating regulators are used. Routing tasks are carried out using

machine-learning techniques, which are also used to forecast the movement and tracking of mobile robots. As one of the largest and most popular subfields of artificial intelligence, learning the machine organizes and investigates the means and procedures by which systems and computers may learn; computer programs can gradually enhance their performance in response to input [5]. Evolutionary algorithms and subsets of these swarm intelligence algorithms are among the approaches taken into account in the routing and tracking of missiles and are a member of the machine learning family. A systematic characteristic of swarm intelligence is that the agents cooperate locally and that their overall behavior converges to a location somewhat near the best solution. These algorithms' strength is the lack of a global control. This part takes a fast overview for UAVs controller based on target trajectory and path scheduling. [6]

MPC used in several systems. A new form of PD controller proposed for dynamic positioning system, which used adaptive dynamic modeling and programming in time-based form. This controller proposed in the presence of some parameters such as undefined system dynamics and maintaining energy efficiency. In [7], a predictive observer controller based on Lyapunov–Krasovskii proposed for UAVs for collecting some future agent's states. Another article proposed adaptive predictive controller in a system (image-based visual servoing or IBVS system) with disturbance observer [8]. A predictive control model in the form of motion-based used in [9] through LSTM as deep recurrent neural network in ship system. PID used in the form of predictive controller for dynamic positioning system which combined with LSTM algorithm. There are several controllers such as PD, PID and LQR considered in UAVs. In [10] UAV flight control and position recognition in flight time optimized due to reducing time in controller.

Aerodynamics in constant forms based on Lyapunov theory is one of the key controller parameters for system dependability. Also proportional, derivative and integral control methods proposed in [11] for smart controllers. Advances in theorizing of control systems led to introducing smarter controller by using fuzzy logic, neuro-fuzzy and neural controllers which can affected a tremendous impact by combining proportional, derivative and integral mode in other controllers. In [12] a derivative-proportional controller designed for path trajectory and external disturbance reduction.

The ideal input signal proposed from changeable feedback used in controller systems is one benefit of the

---

<sup>2</sup> HMM

LQR controller [13]. On the other hand, PID controllers for four-rotor UAVs were optimized with evolutionary and swarm intelligence techniques such as PSO, HSA, and GA, with PSO achieving the best results [14]. A vision-based controller proposed in [15] for UAVs based on neural networks. MLP neural networks used in this method for target trajectory and navigation.

A new optimal controller proposed in multi rotor UAVs in robust forms [16]. This controller tested with Lyapunov stability model o guaranty the robust form. Also, in [17] an optimal controller in 6-Degree of Freedom (6DOF) of AE2 UAVS proposed to show the performance in wind disturbances condition. The controller was based on feedback linearization. A new back-stepping controller with some constrain proposed for 6-DOF UAVs in adaptive form [18]. Another back-stopping controller proposed for fixed wing UAVs with external disturbance in landing with dynamic inversion [19]. A novel back-stepping controller paradigm based on the adaptive sliding mode in quadrotor UAVs was also suggested in [20]. A novel PID nonlinear controller with six degrees of freedom is utilized in quadrotor UAVs and is optimized via genetic algorithms [21]. For UAVs represented using the dynamic inversion approach, the primary strategy in [22] uses the RISE.

In [23] an observer-based controller proposed for UAVs to disturbance rejection. A new method used in this article named PPF which combined with observed based controller. Another observer-based controller for UAVs proposed in [24] which can extend any states of observer for reducing wind disturbance. Integrating finite time with observer as wind disturbance rejection for UAVs proposed in [25] which obtained better robustness hat recent methods. Controlling multiple UAVs by one predictive controller for virtual guiding to reach to targets proposed in [26] based on MPC. In [27], reinforcement learning combined with MPC for design a new controller for UAVs in robust form.

In [28], proposed three steps level of UAVs planning and trajectory which use GA, ACO and Voronoi diagram with good results of checkpoint. Also, in [29], an experimental model with physical testing proposed which use bio-inspired algorithms for path scheduling and target trajectory. This article impellent the model in real world and also in 3d simulation. Some UAVs used in disaster places of nature for target trajectory and path scheduling which one of them proposed in [30]. This article uses a kind of Genetic algorithm named DEA. In [31], deep learning model used for UAVs target trajectory for optimizing evaluation cost. A new swam intelligence algorithm name SMO used for UAVs target trajectory and planning based on gradient mode with great performance [32].

### 3. Proposed Approach

We use TTR VTOL UAV as main UAV system. The main parameters of TTR VTOL UAVs illustrated in Fig. 1.

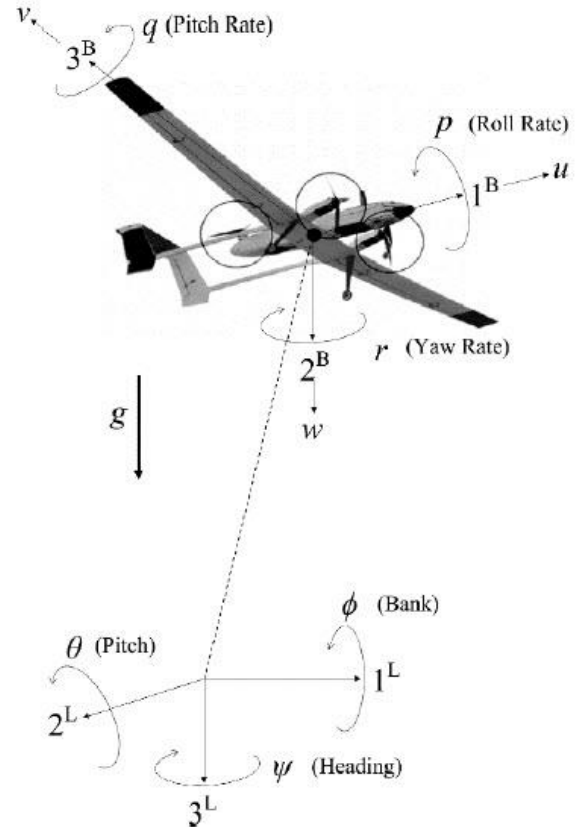


Fig. 1. TTR VTOL UAV main parameters

The prediction of UAVs motion and tracking is a nonlinear optimization problem. The main purpose of tracking the UAVs is to move correctly without dealing with obstacles in the path and adjusting the control variables to optimize one or more objective functions, while at the same time, a series of tracking constraints such as route finding and route shortening. The UAV's tracking problem is mathematically formulated in the form of Eq. (1).

$$\begin{aligned} & \text{Min Func}(x;u) \\ & \text{Subjected to: } h(x;u) \leq 0 \\ & \text{and } g(x;u) = 0 \end{aligned} \quad (1)$$

According to Eq. (1), Func is the objective function that needs to be optimized, h is the inequality constraint that represents the limitations of the UAVs tracking agent, g is the constraints equal and is represented by the non-linear equation  $g(x;u)$  and  $x$  is the vector of independent variables or state variables, and  $u$  the vector of control variables or independent variables. The control variables including the output manufacturer include:

- ✓  $P_G$  is the real power of routing,
- ✓  $P_{G1}$  is the simple route tracking mode,
- ✓  $V_G$  is the UAVs manufacturer's voltage in tracking,
- ✓  $T_S$  is setting the UAVs transmission route,
- ✓  $Q_C$  is the UAVs shunt compensator is in tracking.

Due to the control variables in the tracking of the UAVs, there is Eq. (2).

$$U^T = [P_{G2} \dots P_{G_{NG}} \cdot V_{G1} \dots V_{G_{NG}} \cdot T_{s1} \dots T_{s_{NT}} \cdot Q_{C1} \dots Q_{C_{NC}}] \quad (2)$$

According to Eq. (2), NG, NT, and NC, respectively include path generator numbers, UAVs routing set numbers, and robot UAVs power compensation numbers. The longitudinal motion of the UAVs is examined in this study to monitor routing activities. The UAVs math model is also needed to allow other operations to be performed. The equation of longitudinal motion of a UAVs can be represented by Eq. (3) for linear motion.

$$\begin{pmatrix} \dot{u} \\ \dot{w} \\ \dot{q} \\ \dot{\theta} \\ \dot{h} \end{pmatrix} = \begin{pmatrix} Xu & Xw & Xq & -g\cos(\theta) & 0 \\ Zu & Zw & Zq & -g\sin(\theta) & 0 \\ Mu & Mw & Mq & 0 & 0 \\ 0 & 0 & 1 & 0 & 0 \\ -\sin(\theta) & -\cos(\theta) & 0 & 1 & 0 \end{pmatrix} \begin{pmatrix} u \\ w \\ q \\ \theta \\ h \end{pmatrix} + \begin{pmatrix} X_{\delta_e} & X_{\delta_t} \\ Z_{\delta_e} & 0 \\ M_{\delta_e} & 0 \\ 0 & 0 \\ 0 & 0 \end{pmatrix} \begin{bmatrix} \delta_e \\ \delta_t \end{bmatrix} \quad (3)$$

Which according to Eq. (3),  $t = u\sin(\theta) + w\cos(\theta)$ ,  $\delta_e$  and  $\delta_t$ , are elevators and control inputs of the UAVs,  $u$  is the forward speed (horizontal) of the UAVs,  $w$  is the UAVs vertical speed,  $q$  is the ground and ground rates for the initial UAVs propulsion,  $\theta$  is the ground angle and  $h$  is the UAVs height to the ground, and  $Xu$ ,  $Xw$ ,  $Xq$ ,  $Zu$ ,  $Zw$ ,  $Zq$ ,  $Mu$ ,  $Mw$ , and  $Mq$  as well as  $X_{\delta_e}$ ,  $X_{\delta_t}$ ,  $Z_{\delta_e}$  and  $M_{\delta_e}$  are the later derivatives UAVs stability. The mathematical model in Eq. (3) can be represented by the form of Eq. (4).

$$\dot{x} = Ax + Bu \quad (4)$$

According to Eq. (4),  $x^T = [u \ w \ q \ \theta \ h]$  is the vector of the longitudinal motion of the UAVs, and the Eq. (5), is the transition matrix of the UAVs, as well as the Eq. (6), the distribution of control with the 3D Kalman filter, and  $u^T = [\delta_e \ \delta_t]$ , is the input vector of the control.

$$A = \begin{bmatrix} Xu & Xw & Xq & -g\cos(\theta) & 0 \\ Zu & Zw & Zq & -g\sin(\theta) & 0 \\ Mu & Mw & Mq & 0 & 0 \\ 0 & 0 & 1 & 0 & 0 \\ -\sin(\theta) & -\cos(\theta) & 0 & 1 & 0 \end{bmatrix} \quad (5)$$

$$B = \begin{bmatrix} X_{\delta_e} & X_{\delta_t} \\ Z_{\delta_e} & 0 \\ M_{\delta_e} & 0 \\ 0 & 0 \\ 0 & 0 \end{bmatrix} \quad (6)$$

The stability of the UAVs model has to be examined now. In theory, the transfer function, which is Eq. (7), may be used to derive the longitudinal equations.

$$(s^2 + 15.043s + 78.0719) \left( \frac{s^2 + 0.587s}{+1.1174} \right) = 0 \quad (7)$$

UAVs needs to recognize state space which is modeled as  $q(m+1) = Ax(k) + B\Delta u(m) + \Psi(m)$  and  $y(m:k) = AB(m)$ , where  $u(m)$  is the control input,  $q(m)$  is the state at time step  $m$ ,  $y(m:k)$  is the output, and  $\Psi(m)$  is an unknown disturbance. These equations allowed the system matrices  $A$  and  $B$  to be derived for a single axis with pitch or roll running at 10 Hz such as:

$$A = \begin{bmatrix} 1.0 & 0.1 & 0.0048 & 0.0001 & 0.0010 \\ 0 & 1.0 & 0.0921 & 0.0037 & 0.0397 \\ 0 & 0 & 0.7815 & 0.0614 & 1.0980 \\ 0 & 0 & -3.6435 & 0.2692 & 18.3076 \\ 0 & 0 & 0 & 0 & 1.0 \end{bmatrix}$$

$$B = [0 \ 0.0029 \ 0.2095 \ 9.9251 \ 1.0]^T$$

And state vector is as  $\dot{x} = (p_x \ v_x \ \theta \ \dot{\theta} \ u_x \ p_y \ v_y \ \phi \ \dot{\phi} \ u_y)^T$  based on  $A$  and  $B$ . Output can estimate and calculate in position of  $y = (p_x \ p_y)$ . Other states include some other operator and variables such as velocity ( $v_x, v_y$ ), pitch  $\theta$ , roll  $\phi$  and also their derivatives which stored controls as  $(u_x(m) \cdot u_y(m))$ . In this research, LQG controller is considered as the optimal control method in the UAVs. The vector of optimum control for a system with a state space model under Eq. (8) is as follows:

$$u(t) = -Kx(t) \quad (8)$$

The cost function, also known as the quadratic performance index function, is minimized using Eq. to discover the best control inputs while optimizing state variables at a given moment (9).

$$J = \frac{1}{2} \int (x^T Q x + u^T R u) dt \quad (9)$$

By Eq. (9),  $Q$  is a positive semi-symmetric matrix with definite symmetry, and  $R$  is a positive definite symmetric matrix. Any efficient control is chosen using weight  $Q$  and  $R$  matrices depending on effectiveness. The Gain vector matrix of optimal control is calculated as Eq. (10).

$$K = T^{-1}(T^T)^{-1}B^T P = R^{-1}B^T P \quad (10)$$

Therefore, based on Eq. (10), the optimal control equation is converted into Eq. (11).

$$A^T P + PA - PBR^{-1}B^T P + Q = 0 \quad (11)$$

The UAVs will move in the manner of Eq. (12) stable movement if a definite P positive matrix can be derived using the rational equation

$$A^T P + PA - PBR^{-1}B^T P + Q = 0 \quad (12)$$

Based on a series of specific circumstances, the LQG controller can be designed using a rational equation such as Eq. (11) that can be used without changing the control matrix and mode to find the optimal Gain matrix. The optimized 3D Kalman filter can also be determined by considering that there are several unspecified modes. For a UAVs without adding an integer, we can use the earlier defined matrix A and B to control it by means of a control, and the matrices of the weight of the mode Q and G are used to find the optimal matrix or K, which allows the input of the control gives  $u = -kx(t)$ . In this research, the LQG controller was designed without affecting measurement impediments in the estimation and tracking of UAVs targets. The equations of the system have been discontinued using Euler's approach. Initially, the LQG controller was evaluated without affecting the disturbances, and then the system response to the controller under conditions of disturbance would be investigated, once using the Kalman filter, three-dimensional, and once without using it. Also, operations for estimating and tracking the UAVs target will be carried out during routing time and reach. A three-dimensional Kalman filter will use state equations, and initial values for calculating gain and residual values, as well as estimating the actual value of the signal in the estimation and target tracking. Equations (13) and (14) in the form of linear discrete states and measurement equations are used to analyze the stages of the 3D Kalman filter.

$$X(k+1) = AX(k) + Bu(k) + Gw(k) \quad (13)$$

$$y(k) = HX(k) + v(k) \quad (14)$$

According to the equation of state in Eq. (13), X(k) is the UAVs mode vector, A stands the UAVs propulsion matrix, u(k) shows the UAVs input vector, w(k) is the random Gaussian noise vector with zero mean and covariance structure, B is the control distribution matrix, G is the UAVs noise transmission matrix, which is Gaussian noise. In the equation of measurement, according to Eq. (14), y(k) is the measurement vector, H is the measurement matrix, v(k) is the measured noise vector with mean zero and the covariance structure. There is no relationship between the noise of the UAVs w(k) and the measurement noise v(k). The covariance matrices for w(k) and v(k) are also calculated as Eq. (15) and (16) respectively.

$$E[w(k)w^T(j)] = Q(k)\delta(kj) \quad (15)$$

$$E[v(k)v^T(j)] = R(k)\delta(kj) \quad (16)$$

According to the above two equations,  $\delta(kj)$  is the Kroenke symbol, and E is the expected value. The optimal Three-Dimensional Kalman filter, which estimates the UAVs mode vector, is carried out with the returning equations that follow. The extrapolation equation is calculated by Eq. (17).

$$X_e\left(\frac{k}{k}-1\right) = AX_e\left(\frac{k-1}{k-1}\right) + BK_{LQG}(k-1)(X_d - X_e\left(\frac{k-1}{k-1}\right)) \quad (17)$$

This sequence is shown in general and summary in Eq. (18).

$$\Delta(k) = Z(k) - HX_e\left(\frac{k}{k}-1\right) \quad (18)$$

Also estimates the state calculated by Eq. (19).

$$X_e\left(\frac{k}{k}\right) = X_e\left(\frac{k}{k}-1\right) + K(k)\Delta(k) \quad (19)$$

The Gain matrix of the optimal Three-Dimensional Kalman filter is also calculated from Eq. (20).

$$K(k) = P\left(\frac{k}{k}\right)H^T R^{-1}(k) = P\left(\frac{k}{k}-1\right)H^T \left(HP\left(\frac{k}{k}-1\right)H^T + R(k)\right)^{-1} \quad (20)$$

The covariance matrix of the Three-Dimensional Kalman filter error is also calculated by Eq. (21).

$$P\left(\frac{k}{k}\right) = (I - K(k)H)P\left(\frac{k}{k}-1\right) \quad (21)$$

The covariance matrix of the extrapolation error is also calculated by Eq. (22).

$$P\left(\frac{k}{k}-1\right) = AP\left(\frac{k-1}{k-1}\right)A^T + BD_u(k-1)B^T + GQ(k-1)G^T \quad (22)$$

According to Eq. (18) to (22),  $X_d$  is the arbitrary vector, and I is the identification matrix. The 3D Kalman filter attempts to evaluate the actual signal amount in the target tracking and its estimation with UAVs -based disturbances based on the Dragonfly-Firefly algorithm that is carried out through the Gaussian distribution. These two algorithms have the same operators and application, but their population is different and also fitness function which refer to Eq. (1).

The Dragonfly-Firefly algorithm apply for optimizing path scheduling and target trajectory area. Variation in light intensity or brightness and the formulation of appeal are two crucial components of the Dragonfly-Firefly algorithm. For the sake of simplicity, it is assumed that the brightness of the Dragonfly-Firefly, which is connected to the coding target function, determines how enticing it is. The brightness for firefly with variable I is chosen in the particular location x as  $I(x) \propto f(x)$  to optimize the

optimization of the problems. Other light worms or dragonflies frequently comment on how attractive  $\beta$  is. As a result, there will be a variation in the distance  $r_{ij}$  between firefly or dragonflies  $i$  and  $j$ . It is important to remember that when the light gets further from its sources, its intensity drops. In the simplest scenario, the inverse square law's definition of Eq. (23) is used to determine how the intensity of light  $I(r)$  varies.

$$I(r) = \frac{I_s}{r^2} \quad (23)$$

Where the source of  $I_s$  is strong. For a particular media, the variable  $\gamma$  is used to take into account a consistent light absorption coefficient. With  $r$ , whose relationship is specified by Eq. (24), the brightness  $I$  has a varied intensity.

$$I = I_0 e^{-\gamma r} \quad (24)$$

$I_0$  is the primary brightness's intensity as determined by Eq. (24). The impact of the inverse square law approximation and Gaussian absorption is specified in  $I_s/r^2$  to prevent the singularity mode at  $r=0$  as seen in Eq. (25).

$$I(r) = I_0 e^{-\gamma r^2} \quad (25)$$

The light intensity that fireflies and dragonflies can see directly relates to their appeal. Eq. (26) may be used to describe firefly attraction  $\beta$ .

$$\beta = \beta_0 e^{-\gamma r^2} \quad (26)$$

$\beta_0$  represents attractiveness when  $r=0$  in equation (25). In terms of computing, equation  $1/(1+r^2)$  performs better than the power function, which is often written as Eq. (27).

$$\beta = \frac{\beta_0}{1 + \gamma r^2} \quad (27)$$

A uniformly reducible function, such as Eq. (28), can represent the endearing function  $\beta(r)$  and a Cartesian distance, such as Eq.(29), separates the fireflies/dragonflies  $i$  and  $j$  in  $x_i$  and  $x_j$ .

$$\beta(r) = \beta_0 e^{-\gamma r^m}, \quad (m \geq 1) \quad (28)$$

$$r_{ij} = ||x_i - x_j|| = \sqrt{\sum_{k=1}^d (x_{i,k} - x_{j,k})^2} \quad (29)$$

In the equation (29),  $x_{i,k}$  is the  $k$ 'th spatial coordinate component  $x_i$  and the  $i$ -th firefly/dragonfly. It is represented as Eq. (30) in a two-dimensional mode comparable to Euclidean distance.

$$r_{ij} = \sqrt{(x_i - x_j)^2 + (y_i - y_j)^2} \quad (30)$$

A type of attraction for the firefly/dragonfly  $j$  is provided by the velocity of the insects, as shown by Eq. (31). It is visible with periodic signals, referred to as optimum route scheduling.

$$x_i = x_i + \beta_0 e^{-\gamma r_{ij}^2} (x_j - x_i) + \alpha \epsilon_i \quad (31)$$

Due to the draw of the firefly/dragonfly, Eq. (31)'s second component is required.  $\alpha$  is a randomly chosen parameter, and  $\epsilon_i$  is a vector of randomly chosen values selected from the uniform or Gaussian distribution. According to the degree of fitness of each worm's position, the amount of light emitted at each occurrence is calculated. The quantity of fitness determines how much light is added in each cycle. For each usage, the correlation of the light firefly adjustment is stated as Eq. (32).

$$\varphi_i(t) = (1 - p)\varphi_i(t - 1) + \gamma j(x_i(t)) \quad (32)$$

In Eq. (32), where  $p$  and  $\varphi$  are fixed quantities for simulating the progressive decline and its impact on light,  $j(x_i(t))$  is the new value of the firefly's light-emitting at reuse time, and  $(1 - p)\varphi_i(t - 1)$  is the fitness location of the worm  $I$  in the repetition  $t$  of the algorithm. Eq (33) is employed to pinpoint the target trajectory or determine the nearby location of other worms.

$$p_{ij}(t) = \frac{\varphi_j(t) - \varphi_i(t)}{\sum_{k \in N_i(t)} \varphi_k(t) - \varphi_i(t)} \quad (33)$$

In Eq. (33),  $N_i(t)$  is the set of fireflies from firefly neighboring at time  $t$ . There is a gap between the firefly  $i$  and  $j$  at time  $t$  which essentially use Euclidean distance as  $d_{ij}(t)$ . The probability  $p$  of Eq. (34) may be used to solve the firefly's arbitrary time shift.

$$x_i(t + 1) = x_i(t) + s \left( \frac{x_j(t) - x_i(t)}{||x_j(t) - x_i(t)||} \right) \quad (34)$$

In the Eq. (34), the operator  $||\dots||$  displays the Euclidean soft function and  $s$  is the step of motion.  $x_i(t)$  is the  $m$ -dimensional vector of the firefly/dragonfly location in the time unit  $t$ . Updating data neighbors with duplicate phrases is also another matters, and the need to updating neighbor range is felt. For any firefly/dragonfly,  $i$  is assigned a neighbor, whose radial range  $r_d^i$  is naturally dynamic. According to Eq. (35), neighboring update operations are obtained.

$$r_d^i(t + 1) = \min \{r_s, \max \{0, r_d^i(t) + \beta(n_t - |N_i(t)|)\}\} \quad (35)$$

In Eq. (35),  $\beta$  is a constant parameter and  $n_t$  is a parameter to control the number of neighborhoods or to identify the exact areas for trajectory.

#### 4. simulation

Given the fact that various parameters for different parts of the UAV are mentioned in this study, at the beginning of the simulation, the set values should be noted.

Inputs in this control include speed, type of longitudinal or deep motion, torque and route identification, and output is path detection and target tracking. In the beginning, different parameters of a UAV can be found in Table (1).

**Table 1.** Specification of studied DGs.

UAV rotational capability	$\pi/180$
m/s <sup>2</sup> ( Gravity)	9.81
Frequency (Hz)	60
m/s( Light Speed)	299792458
Boltzman Constant	17
Sampling rate for simulation (specific for Euler integral) - (sec)	0.5
Fly Time (sec)	270
Environment Size (Km)	12x12
UAV cruiser height (m)	200
Average speed at flight time (m/s)	30
Minimum speed at flight time (m/s)	15
Maximum speed at flight time (m/s)	50
Spin speed in radius (m/s)	200
Initial UAV gain	1
Path to goal (m)	2500
Internal engine heat engine UAV (centigrade)	23

Similarly, the parameters of the Bat Algorithm are according to Table (2).

**Table 2.** Dragonfly-Firefly Algorithm Parameters

Iteration Number	1000
Initial Population of dragonflies/fireflies	1
Light intensity rate	0.3
Attraction rate	2

When the simulation is performed, the longitudinal motion of the UAV first shows its output. Fig. 2, divided into four sections, shows the response of each step of the

UAV movement from the onset of flight from the ground to the steady, stable level of flight in the sky.

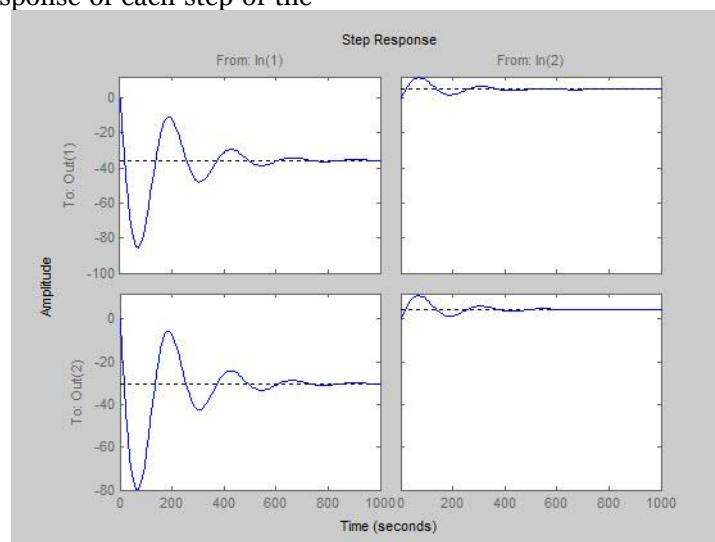




**Fig. 2.** Shows the UAV output from the beginning of the flight to the equilibrium point in flight in the sky

Depending on the Fig. (2) and the settings made for the UAV, it is shown how the UAV moves at any moment. In all the domain images, from the time of flight to reaching a specific point, is shown. On the upper left, the UAV range is shown initially, which is intended to move from the ground. In the upper left-hand figure, the range of motion

is shown from the surface of the ground, reaching a given point of flight. In the lower left-hand figure, the range of balance adjustment is shown on the fly. In the bottom right-hand side, the equilibrium point is shown. Based on this range of motion adjustment, four Fig. (3) to (6) are also shown for setting conditions.

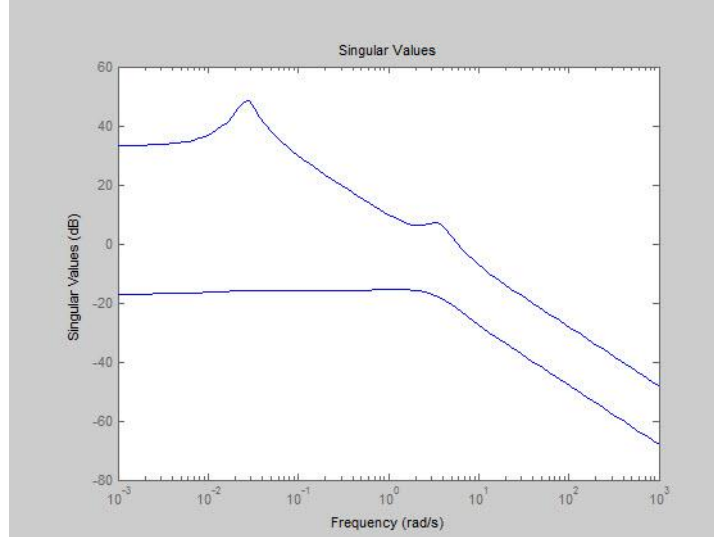


**Fig. 3.** UAV range with the intention of moving from the ground

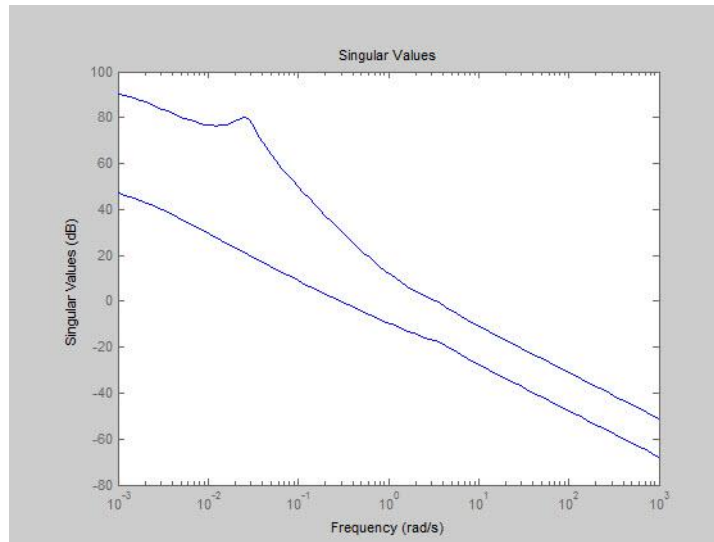


**Fig. 4.** The range of motion from the ground to a specific point of flight

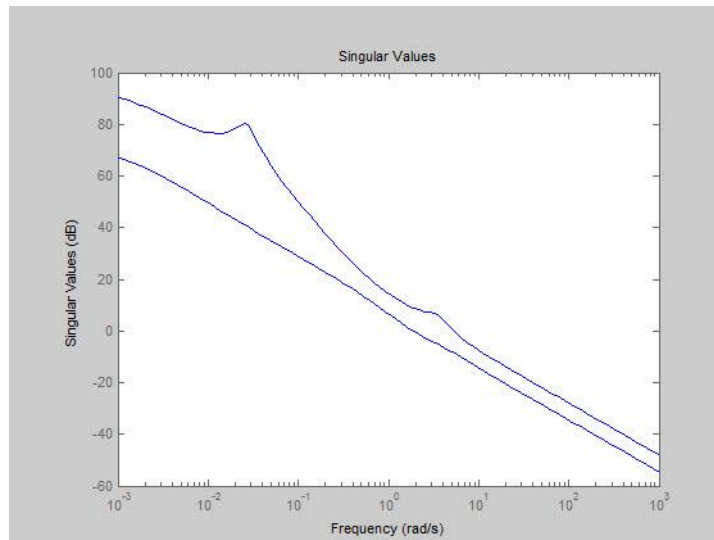


**Fig. 5.** Flight adjustment range

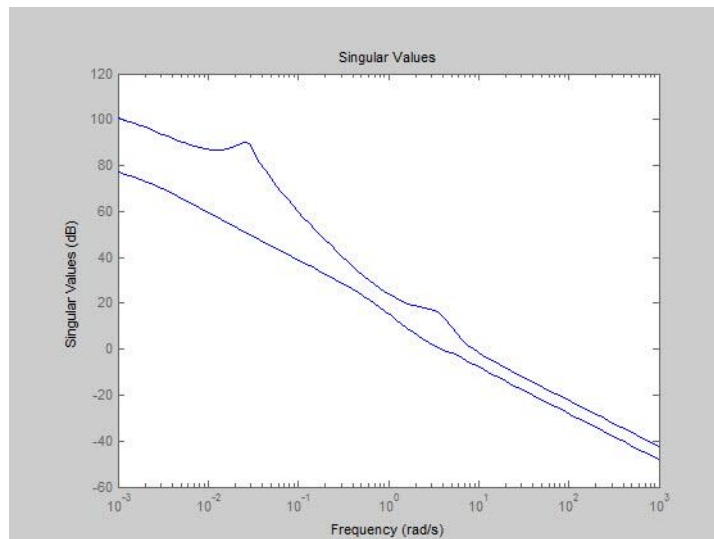


**Fig. 6.** Reaching the range of the equilibrium point

The stable mode is also shown in Fig. (7) after applying the motion. This section will be based on the LQG controller. Given this shape, it can be seen that the UAV is in perfect balance and the controller provided in the UAV is

resistant to the settings. According to Fig. (7), it can be seen that the rate of delay in moving UAV is commensurate with the flight time to reach the target and is declining.

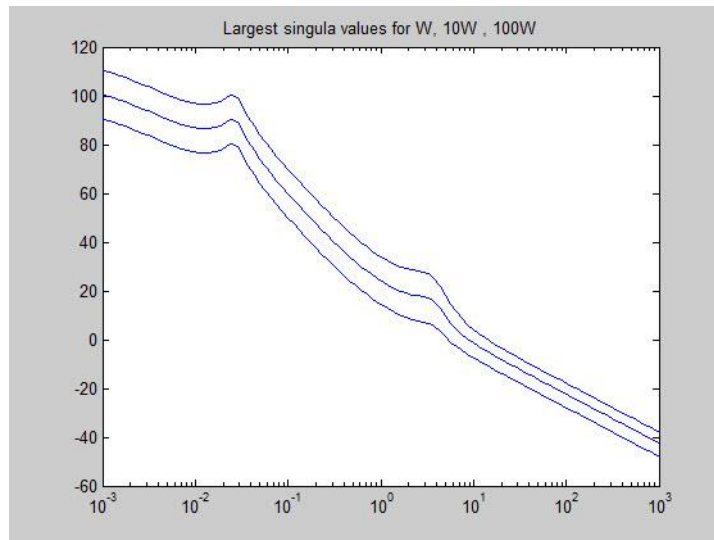


**Fig. 7.** Rate of delay in UAV movement

After the operation, the UAV output will be shown. The graphical form of it for moving in an environment of a given path is based on a LQG controller based on a Three-Dimensional Kalman filter based on the Dragonfly/Firefly algorithm and the property that has all evolutionary algorithms and swarm intelligence being randomly and

may be in each run time from a path, move and start moving to reach the target. But the prediction of moving and tracing it with this algorithm is constant and tracks it until it reaches the target. In Fig. (8), we can see the path scheduling and target trajectory in real-time mode in graphical output.

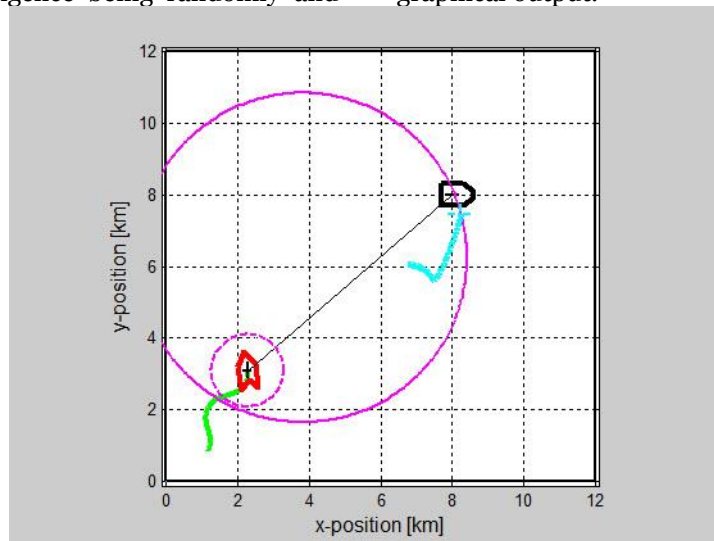


**Fig. 8.** The initial movement of the UAV at a specified path and tracing it to reach the target

According to Fig. (8), the UAV will move in a 12x12 km environment. The D spot, which is specified at 8x8 km coordinates, is the main objective that the UAV must take to reach its path. This is a path traversal using the routing, modeling and its outputs are shown in Fig. (2) and below, from Fig. (3) to Fig. (4), and eventually reaching a state

balance was flying and resistant in Fig. (7). The UAV is shown in red color. The green lines are the UAV path. There are two pink circular lines, one spotted near the UAV which detects the motion of an UAV to track the target or D and tracks in real-time mode for any movement of the UAV. Also, the large pink circle performs route estimation

according to the direction the UAV runs. Initially, this is a large circle and, to reach the target, it will be as small as possible until the estimated operation is done correctly.

Several illustrations of the UAV outputs to reach the target are shown in Fig. (9) to (12).

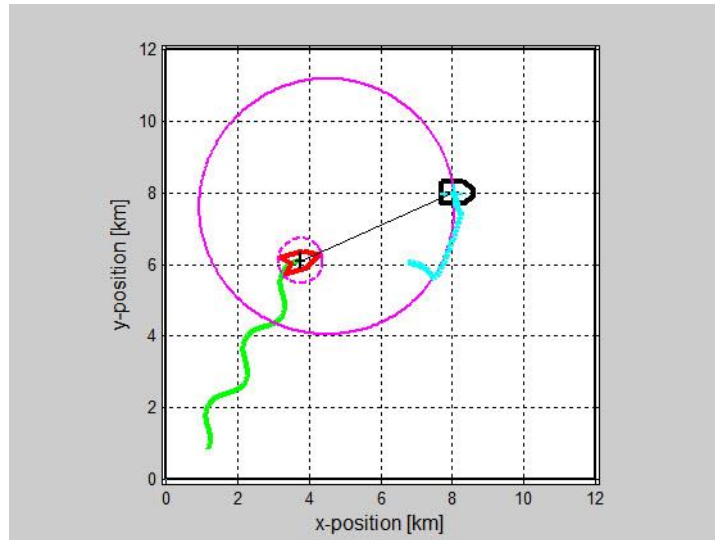


**Fig. 9.** Shows the movement of the UAV from the green path and tracing and estimating the target

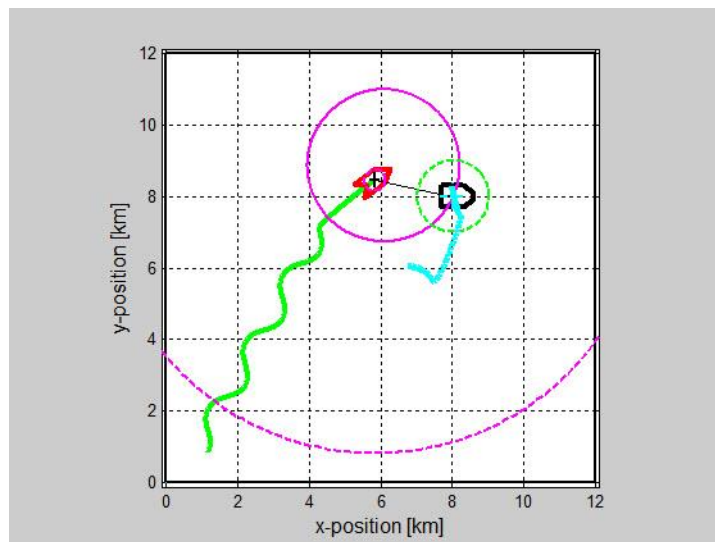


**Fig. 10.** Shows the movement of the UAV from the green path and tracking and target estimation - approaching the target or D

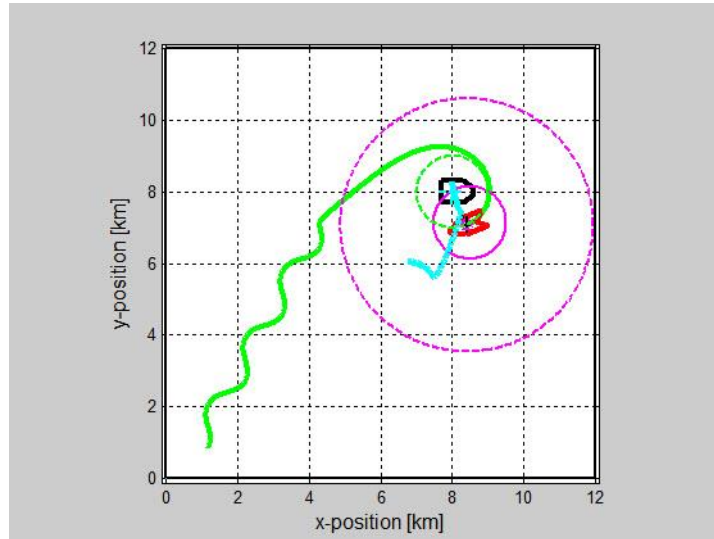


**Fig. 11.** Shows the movement of the UAV from the green path and tracing and objective estimation - crossing the green circle of the dots around the target or D

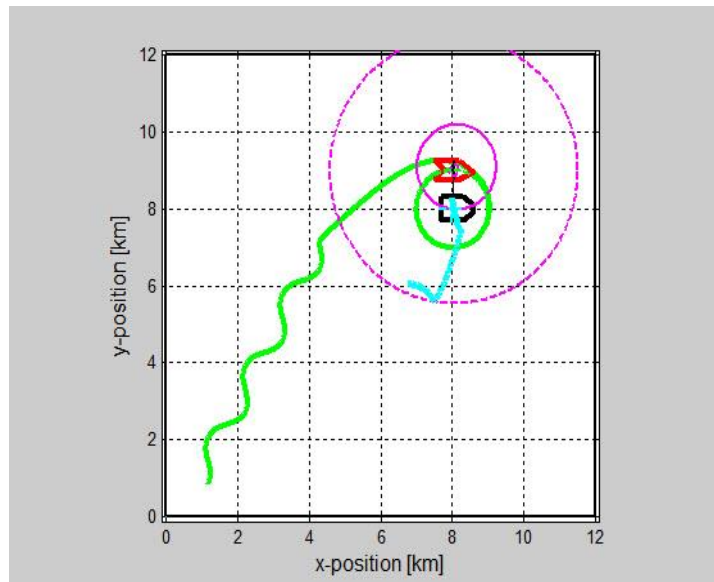


**Fig. 12.** Finishing the simulation and passing a specific path to the goal with its tracking and estimating

The UAV power consumption is equivalent to 56.2045 mW at the simulation's conclusion, indicating a successful passing. MSE, PSNR, SNR, and Accuracy Criteria will all be employed as assessment criteria in this study. After the project is completed, it is possible to guarantee that the

suggested approach will be utilized for UAV route scheduling and target trajectory optimization based on the findings of the assessment criteria. The outcomes of the evaluation techniques are displayed in Table 3.

**Table 3.** Outcomes of evaluation criteria

Specificity (%)	Sensitivity (%)	Accuracy (%)	SNR (dB)	PSNR (dB)	MSE
80.07	80.08	96.00	56.0618	9.9310	0.6400

## 5. Conclusion

The UAV tracking is known as an important issue in military science. Today, the design of UAVs is tracked to reach and reach targets, and are capable of controlling and redirecting. The proposed approach of this study is to use evolved methods to track UAVs until the goal is achieved. For this purpose, after modeling the UAV system and positioning and deploying it, the specified and the same path are proposed as an optimization space. Simulation findings show that the UAV's power consumption is equivalent to 56.2045 mW. The UAVs tracking route uses a combination of LQG controller with 3D Kalman filter for tracing, but due to no real-time tracing and path scheduling, a new combinational method apply which is Dragonfly/Firefly algorithm. In the future plans, we try to make a simulation of the proposed approach and prove it and compare it with the basic articles of this research.

## REFERENCES

- [1] Y.-W. Fang, D.-D. Qiao, L. Zhang, P.-F. Yang, and W.-S. Peng, "A new cruise missile path tracking method based on second-order smoothing," *Optik (Stuttg)*, vol. 127, no. 12, pp. 4948–4953, 2016.
- [2] S. Qiao, D. Shen, X. Wang, N. Han, and W. Zhu, "A self-adaptive parameter selection trajectory prediction approach via hidden Markov models," *IEEE Transactions on Intelligent Transportation Systems*, vol. 16, no. 1, pp. 284–296, 2014.
- [3] M. Soltani, M. Keshmiri, and A. K. Misra, "Dynamic analysis and trajectory tracking of a tethered space robot," *Acta Astronaut*, vol. 128, pp. 335–342, 2016.
- [4] Y. O. Mohammed and A. J. Alzubaidi, "Extended Kalman Filter based Missile Tracking," *International Journal of Computational Engineering Research*, vol. 4, no. 4, pp. 16–18, 2014.
- [5] F. Barboza, H. Kimura, and E. Altman, "Machine learning models and bankruptcy prediction," *Expert Syst Appl*, vol. 83, pp. 405–417, 2017.
- [6] F. T. Shahdoost, "Adaptive Fuzzy Sliding Mode based on Model Predictive Control in UAV's Robot using Optimized Deep Learning Approach".
- [7] J. Wang, Z. Zhou, C. Wang, and Z. Ding, "Cascade structure predictive observer design for consensus control with applications to UAVs formation flying," *Automatica*, vol. 121, p. 109200, 2020.
- [8] Z. Qiu, S. Hu, and X. Liang, "Disturbance observer based adaptive model predictive control for uncalibrated visual servoing in constrained environments," *ISA Trans*, vol. 106, pp. 40–50, 2020.
- [9] D. Lee and S. J. Lee, "Motion predictive control for DPS using predicted drifted ship position based on deep learning and replay buffer," *International Journal of Naval Architecture and Ocean Engineering*, vol. 12, pp. 768–783, 2020.
- [10] S. Haoqin, H. Zhan, B. Xiaoxiang, S. Hongwei, and S. Jing, "Morphing process research of uav with pid controller," *Procedia Eng*, vol. 99, pp. 873–877, 2015.
- [11] J. Li and Y. Li, "Dynamic analysis and PID control for a quadrotor," in *2011 IEEE International Conference on Mechatronics and Automation*, 2011, pp. 573–578.
- [12] T. Sangyam, P. Laohapiengsak, W. Chongcharoen, and I. Nilkhamhang, "Path tracking of UAV using self-tuning PID controller based on fuzzy logic," in *Proceedings of SICE annual conference 2010*, 2010, pp. 1265–1269.
- [13] I. D. Cowling, J. F. Whidborne, and A. K. Cooke, "Optimal trajectory planning and LQR control for a quadrotor UAV," 2006.
- [14] F. T. Shahdoost, "Adaptive Fuzzy Sliding Mode based on Model Predictive Control in UAV's Robot using Optimized Deep Learning Approach".
- [15] D. Maravall, J. de Lope, and J. P. Fuentes, "Vision-based anticipatory controller for the autonomous navigation of an UAV using artificial neural networks," *Neurocomputing*, vol. 151, pp. 101–107, 2015.
- [16] O. A. Jasim and S. M. Veres, "A robust controller for multi rotor UAVs," *Aerosp Sci Technol*, vol. 105, p. 106010, 2020.
- [17] A. K. Tripathi, V. v Patel, and R. Padhi, "Autonomous landing design of uavs using feedback linearization controller with anti windup scheme," *IFAC-PapersOnLine*, vol. 53, no. 1, pp. 81–86, 2020.
- [18] Y. Zhang, S. Wang, B. Chang, and W. Wu, "Adaptive constrained backstepping controller with prescribed performance methodology for carrier-based UAV," *Aerosp Sci Technol*, vol. 92, pp. 55–65, 2019.
- [19] M. Lungu, "Backstepping and dynamic inversion combined controller for auto-landing of fixed wing UAVs," *Aerosp Sci Technol*, vol. 96, p. 105526, 2020.
- [20] M. Labbadi and M. Cherkaoui, "Robust adaptive backstepping fast terminal sliding mode controller for uncertain quadrotor UAV," *Aerosp Sci Technol*, vol. 93, p. 105306, 2019.
- [21] A. A. Najm and I. K. Ibraheem, "Nonlinear PID controller design for a 6-DOF UAV quadrotor system," *Engineering Science and Technology, an International Journal*, vol. 22, no. 4, pp. 1087–1097, 2019.
- [22] S. Y. Vural, J. Dasedemir, and C. Hajiyev, "Passive fault tolerant lateral controller design for an UAV," *IFAC-PapersOnLine*, vol. 51, no. 30, pp. 446–451, 2018.
- [23] J. Chen, R. Sun, and B. Zhu, "Disturbance observer-based control for small nonlinear UAV systems with transient performance constraint," *Aerosp Sci*

- Technol*, vol. 105, p. 106028, 2020.
- [24] K. Guo, J. Jia, X. Yu, L. Guo, and L. Xie, "Multiple observers based anti-disturbance control for a quadrotor UAV against payload and wind disturbances," *Control Eng Pract*, vol. 102, p. 104560, 2020.
- [25] X. Yu, J. Yang, and S. Li, "Finite-time path following control for small-scale fixed-wing UAVs under wind disturbances," *J Franklin Inst*, vol. 357, no. 12, pp. 7879–7903, 2020.
- [26] C. A. I. Zhihao, W. Longhong, Z. Jiang, W. U. Kun, and W. Yingxun, "Virtual target guidance-based distributed model predictive control for formation control of multiple UAVs," *Chinese Journal of Aeronautics*, vol. 33, no. 3, pp. 1037–1056, 2020.
- [27] C. Greatwood and A. G. Richards, "Reinforcement learning and model predictive control for robust embedded quadrotor guidance and control," *Auton Robots*, vol. 43, no. 7, pp. 1681–1693, 2019.
- [28] Y. V. Pehlivanoglu and P. Pehlivanoglu, "An enhanced genetic algorithm for path planning of autonomous UAV in target coverage problems," *Appl Soft Comput*, vol. 112, p. 107796, 2021.
- [29] Z. Yaoming, S. U. Yu, X. I. E. Anhuan, and K. Lingyu, "A newly bio-inspired path planning algorithm for autonomous obstacle avoidance of UAV," *Chinese Journal of Aeronautics*, vol. 34, no. 9, pp. 199–209, 2021.
- [30] X. Yu, C. Li, and J. Zhou, "A constrained differential evolution algorithm to solve UAV path planning in disaster scenarios," *Knowl Based Syst*, vol. 204, p. 106209, 2020.
- [31] Y. Liu, H. Wang, J. Fan, J. Wu, and T. Wu, "Control-oriented UAV highly feasible trajectory planning: A deep learning method," *Aerosp Sci Technol*, vol. 110, p. 106435, 2021.
- [32] Q. Xia, S. Liu, M. Guo, H. Wang, Q. Zhou, and X. Zhang, "Multi-UAV trajectory planning using gradient-based sequence minimal optimization," *Rob Auton Syst*, vol. 137, p. 103728, 2021.